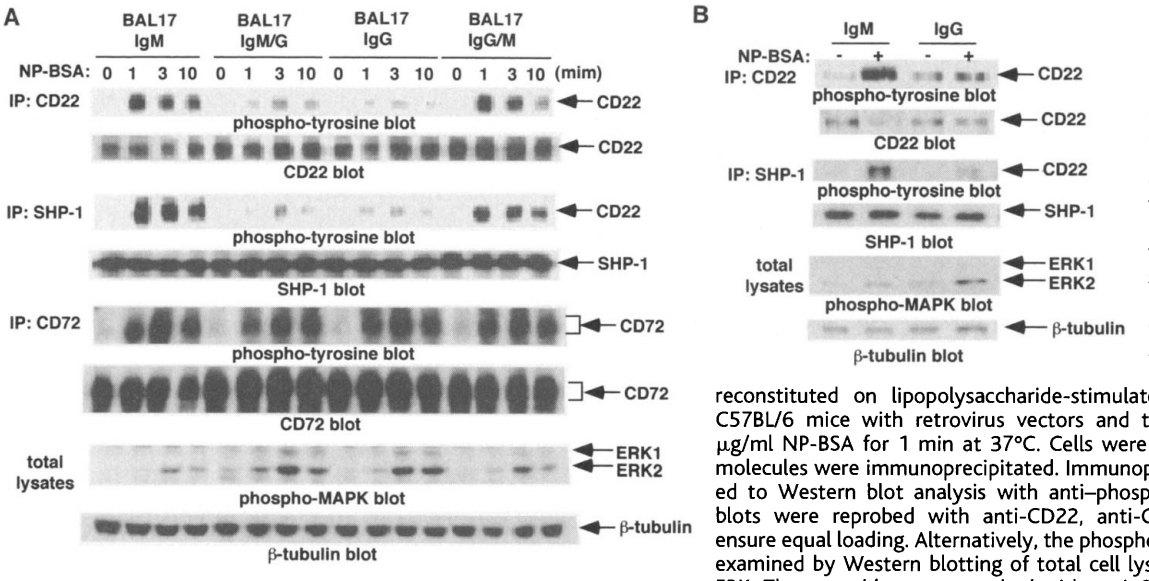

Fig. 4. CD22 regulates BCR signaling in an isotype-specific manner in the B cell line BAL17 and mouse spleen B cells. (**A**) NP-specific IgM-BCR, IgG-BCR, IgM/G chimera, or IgG/M chimera was reconstituted on the B cell lines BAL17 with retrovirus vectors. Infectants were stimulated with 0.2 μg/ml NP-BSA for the indicated times at 37°C. (**B**) Alternatively, NP-specific IgM-BCR or IgG-BCR was reconstituted on lipopolysaccharide-stimulated spleen B cells from C57BL/6 mice with retrovirus vectors and then stimulated with 10 μg/ml NP-BSA for 1 min at 37°C. Cells were lysed, and the indicated molecules were immunoprecipitated. Immunoprecipitates were subjected to Western blot analysis with anti–phospho-tyrosine (4G10). The blots were reprobed with anti-CD22, anti-CD72, or anti–SHP-1 to ensure equal loading. Alternatively, the phosphorylation level of ERK was examined by Western blotting of total cell lysates with anti–phospho-ERK. The same blot was reprobed with anti–β-tubulin to ensure equal loading. Representative data from at least three experiments are shown. Dose-response analysis on BAL17 cells is shown in fig. S5A.

uted to other factors such as their increased affinity to antigens as a result of accumulated somatic mutations of immunoglobulin during the generation of memory B cells (*24*).

References and Notes

1. M. Reth, J. Wienands, *Annu. Rev. Immunol.* **15**, 453 (1997).
2. T. Kurosaki, *Annu. Rev. Immunol.* **17**, 555 (1999).
3. S. W. Martin, C. C. Goodnow, *Nature Immunol.* **3**, 182 (2002).
4. T. F. Tedder, J. Tuscano, S. Sato, J. H. Kehrl, *Annu. Rev. Immunol.* **15**, 481 (1997).
5. L. O'Rourke, R. Tooze, D. T. Fearon, *Curr. Opin. Immunol.* **9**, 324 (1997).
6. T. Tsubata, *Curr. Opin. Immunol.* **11**, 249 (1999).
7. T. Adachi, C. Wakabayashi, T. Nakayama, H. Yakura, T. Tsubata, *J. Immunol.* **164**, 1223 (2000).
8. R. M. Tooze, G. M. Doody, D. T. Fearon, *Immunity* **7**, 59 (1997).
9. C. J. Peaker, M. S. Neuberger, *Eur. J. Immunol.* **23**, 1358 (1993).
10. C. Leprince, K. E. Draves, R. L. Geahlen, J. A. Ledbetter, E. A. Clark, *Proc. Natl. Acad. Sci. U.S.A.* **90**, 3236 (1993).
11. T. L. O'Keefe, G. T. Williams, S. L. Davies, M. S. Neuberger, *Science* **274**, 798 (1996).
12. K. L. Otipoby *et al.*, *Nature* **384**, 634 (1996).
13. S. Sato *et al.*, *Immunity* **6**, 551 (1996).
14. L. Nitschke, R. Carsetti, B. Ocker, G. Kohler, M. C. Lamers, *Curr. Biol.* **7**, 133 (1997).
15. C. Pan, N. Baumgarth, J. R. Pames, *Immunity* **11**, 495 (1999).
16. J. Wienands, J. Hombach, A. Radbruch, C. Riesterer, M. Reth, *EMBO J.* **9**, 449 (1990).
17. P. Weiser, C. Riesterer, M. Reth, *Eur. J. Immunol.* **24**, 665 (1994).
18. G. M. Doody *et al.*, *Science* **269**, 242 (1995).
19. T. Adachi, H. Flaswinkel, H. Yakura, M. Reth, T. Tsubata, *J. Immunol.* **160**, 4662 (1998).
20. Materials and methods are available as supporting material on *Science* Online.
21. M. Reth, *Annu. Rev. Immunol.* **10**, 97 (1992).
22. T. Kaisho, F. Schwenk, K. Rajewsky, *Science* **276**, 412 (1997).
23. C. Wakabayashi, Y. Takahashi, T. Takemori, T. Tsubata, unpublished data.
24. K. Rajewsky, *Nature* **381**, 751 (1996).

25. We thank M. Reth for cell lines and plasmids; L. Nitschke, T. Kitamura, G. Nolan, and H. Yakura for reagents; Y. Takahashi and T. Takemori for sharing unpublished data; and H. Fujimoto, S. Irie, and K. Mizuno for technical help. Supported by grants from the Japanese Ministry of Education, Science, Sport and Culture, and the Mochida Memorial Foundation for Medical and Pharmaceutical Research.

Supporting Online Material
www.sciencemag.org/cgi/content/full/298/5602/2392/DC1
Materials and Methods
Figs. S1 to S5
References and Notes

5 August 2002; accepted 24 October 2002

Photosynthetic Light Harvesting by Carotenoids: Detection of an Intermediate Excited State

G. Cerullo,[1]* D. Polli,[1] G. Lanzani,[1] S. De Silvestri,[1] H. Hashimoto,[2]† R. J. Cogdell[2]

We present the first direct evidence of the presence of an intermediate singlet excited state (S_x) mediating the internal conversion from S_2 to S_1 in carotenoids. The S_2 to S_x transition is extremely fast and is completed within approximately 50 femtoseconds. These results require a reassessment of the energy transfer pathways from carotenoids to chlorophylls in the primary step of photosynthesis.

Light harvesting by carotenoids is a fundamental part of the earliest reaction in photosynthesis (*1–3*). Light energy that is absorbed by carotenoids is rapidly and efficiently transferred to the chlorophylls, thereby allowing photosynthesis to harvest energy over a wider range of wavelengths than would be possible with chlorophyll alone. In some marine environments, major primary producers such as dinoflagellates survive solely on light absorbed by their carotenoids (*4*). Other than their role in photosynthesis, carotenoids are also widely studied as models for conjugated polymers (*5*) and are candidates for molecular electronics applications. Over the past decade, stimulated by the determination of several high-resolution structures of photosynthetic antenna complexes (*6*), there has been great interest in understanding the detailed mechanisms involved in the carotenoid-to-chlorophyll singlet-singlet energy transfer reaction (*3*, *7*). By using ultrafast spectroscopy to probe the very early events of energy relaxation in carotenoids, we directly demonstrate the existence of an intermediate excited state. This requires a reassessment of the current mechanistic description of the accessory light-harvesting function of carotenoids.

[1]National Laboratory for Ultrafast and Ultraintense Optical Science (INFM), Dipartimento di Fisica, Politecnico di Milano, Piazza L. da Vinci 32, 20133 Milano, Italy. [2]Division of Biochemistry and Molecular Biology, University of Glasgow, Glasgow, UK.

*To whom correspondence should be addressed. E-mail: giulio.cerullo@fisi.polimi.it
†Present address: "Light and Control," PRESTO/JST, Department of Physics, Graduate School of Science, Osaka City University, Osaka, Japan.

Classically, carotenoid photophysics has been interpreted in terms of two low-lying excited singlet states, called S_2 ($1^1B_u^+$) and S_1 ($2^1A_g^-$) (*2*). Due to selection rules, the one photon allowed transition from the ground state S_0 ($1^1A_g^-$) goes to S_2, which then internally converts to S_1 in a few hundred femtoseconds (*8–10*). Decay from S_1 to the ground state then occurs in a few picoseconds. Singlet-singlet resonant energy transfer from carotenoids to chlorophylls has been described, depending on the antenna complex involved, as going either from S_2 to the chlorophyll Q_x excited state or from S_1 to the Q_y state (*3*, *7*); in some complexes, both pathways are active (*11*). Theoretical calculations (*12*, *13*) had predicted additional excited states for carotenoids, and recently, they were supported by experimental results suggesting that carotenoids may have an additional excited singlet state (which we call S_x) of $^1B_u^-$ symmetry, lying between S_2 and S_1 (*14–17*). Because of the extremely fast time scales of the processes involved, however, this intermediate state was not directly observed, and its existence was debated.

The recent availability of pulses with 10- to 20-fs duration, tunable throughout the visible and the near infrared, allows us to probe the early events of energy relaxation in carotenoids with unprecedented temporal resolution (*18*). Here, we exploit this improved temporal resolution, to directly monitor the dynamical resolution of the intermediate S_x state.

We studied two carotenoids, β-carotene and lycopene, in cyclohexane solution at room temperature. Both molecules were excited by 15-fs blue pulses centered at 510 nm, resonant with the S_0 to S_2 ($S0 \rightarrow S_2$) transition (*19*), and the temporal evolution of differential transmission was probed in the visible spectral range (500 to 700 nm) using sub–10-fs pulses and in the near-infrared range (820 to 1020 nm) using 12-fs pulses. Pump and probe pulses were derived from two independent non-collinear optical parametric amplifiers (*20–22*).

Figure 1 shows differential transmission spectra in all-*trans*-β-carotene at three different time delays after photoexcitation. After the pump pulse, we observe the prompt appearance of a broad photoinduced absorption (PA) band, extending from 600 to 950 nm; we call this band PA_2. The band decays very quickly and is replaced, within ≈50 fs, by another band (PA_x) peaking at 980 nm; PA_x decays on the 100-fs time scale with a kinetic matching the formation of a new band (PA_1) peaking at 565 nm. The PA_1 band is a well-known feature of carotenoids (*8*, *18*) and is assigned to the $S_1 \rightarrow S_n$ absorption, thus providing a spectral signature of the internal conversion process. The PA_x band was also previously observed (*17*, *23*) and attributed to transient absorption from the S_2 state. These data are at variance with those expected in the classical three-level picture of carotenoid singlet states and indicate the presence of an extra state between S_2 and S_1. We assigned PA_2 and PA_x to transient absorption from the S_2 and S_x states, respectively; the very rapid decay of PA_2 and the corresponding rise of PA_x highlight the initial $S_2 \rightarrow S_x$ conversion process. The subsequent decay of PA_x and rise of PA_1 correspond to the $S_x \rightarrow S_1$ conversion.

This photoexcitation scenario is confirmed by differential transmission dynamics at different probe wavelengths (Fig. 2). At a wavelength of 850 nm (Fig. 2C), we see an instantaneously rising signal, due to the PA_2 band, which decays within 50 fs; at longer times, we observe a tail of the PA_x band, disappearing within ≈ 400 fs. At a wavelength of 980 nm (Fig. 2D), we see the delayed PA_x absorption, with a rise time matching the PA_2 decay and a subsequent decay, over the time scale of a few hundreds of femtoseconds, to form PA_1. The PA_1 band is best monitored at a wavelength of 560 nm (Fig. 2A); it does not rise instantaneously after photoexcitation, but is rather delayed by ≈ 50 fs, in agreement with our kinetic model. At a wavelength of 650 nm (Fig. 2B), we observe, again, at early times a signature of the PA_2 band followed by the slow rise of PA_1. The inset in Fig. 2 shows the initial

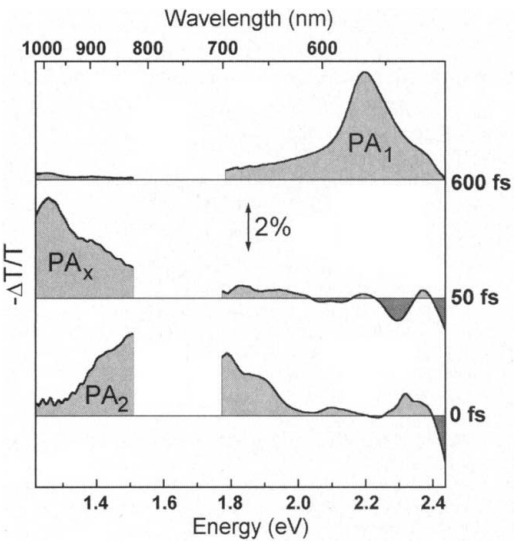

Fig. 1. Differential transmission spectra in all-*trans* β-carotene in cyclohexane solution at different time delays after photoexcitation by a 15-fs pulse resonant with the $S_0 \rightarrow S_2$ transition. A sub–10-fs visible pulse probes the 500- to 710-nm wavelength region, whereas a 12-fs near-infrared pulse probes the 820- to 1020-nm region.

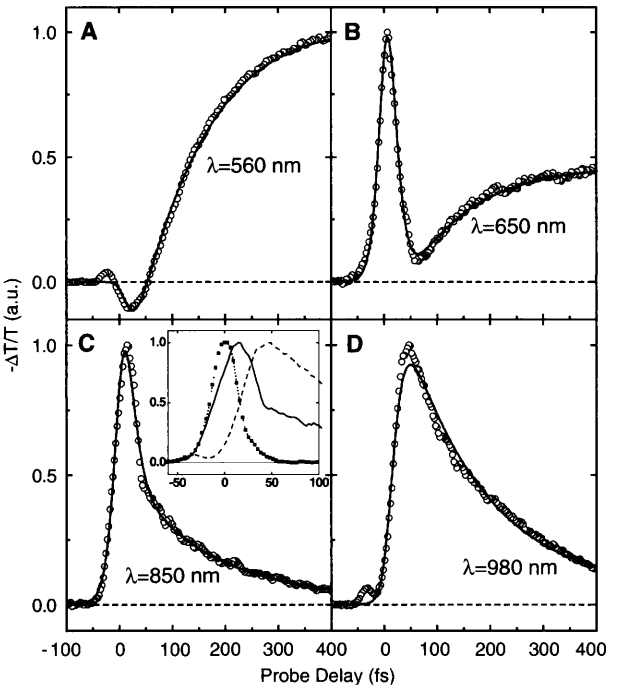

Fig. 2. (**A**) Circles show differential transmission dynamics in all-*trans* β-carotene at 560-nm probe wavelength after photoexcitation with a 15-fs pulse resonant with the $S_0 \rightarrow S_2$ transition. Solid lines are fits obtained using the four-state model described in the text and convoluting the system response with the pump-probe cross-correlation function. (**B**) Same as (A), at 650-nm probe wavelength. (**C**) Same as (A), at 850-nm probe wavelength. (**D**) Same as (A), at 980-nm probe wavelength. The inset in (C) shows the rise times of the signals at 850 nm (solid line) and 980 nm (dotted line), together with a pump-probe cross-correlation (squares).

kinetics of PA_2 and PA_x. On this expanded time scale, the delay in the formation of PA_x relative to PA_2 is clearly seen. The pump-probe cross-correlation illustrates that this delay is well resolved. Figure 2 also shows, as solid lines, exponential fits using a four-level model, which allow us to extract the time constants $\tau_{2x} = 10 \pm 2$ fs for the $S_2 \rightarrow S_x$ conversion process and $\tau_{x1} = 150$ fs for the $S_x \rightarrow S_1$ conversion process (use of rate equations should be considered as a first order approximation to describe the extremely fast $S_2 \rightarrow S_x$ conversion process).

In order to be sure that our observations are applicable to carotenoids other than β-carotene, we extended our experiments to include lycopene. Differential transmission dynamics at relevant wavelengths are reported in Fig. 3. These data can also be explained by introducing an intermediate state; a three-level model is unable to explain the delay in the formation of S_x absorption (980-nm trace) and in the onset of the exponential rise of S_1 absorption (560-nm trace). Exponential fits (solid lines in Fig. 3) give $\tau_{2x} = 9 \pm 2$ fs and $\tau_{x1} = 90$ fs, for lycopene.

Previous studies have used time-resolved fluorescence to monitor the S_2 to S_1 transition in carotenoids (*9*, *10*). Typically the decay of the fluorescence signal from S_2 kinetically matches the rise time of S_1, monitored by the appearance of the $S_1 \rightarrow S_n$ absorption. This was interpreted as strong evidence for the classical three-level model (Fig. 4A). However, theoretical work by Tavan and Schulten (*12*, *13*) on long polyenes had previously calculated the energy levels of a number of so-called "covalent states" lying below the first excited ionic state (S_2). For the backbone lengths relevant to our study, their calculation predicted the presence of an additional low-lying excited singlet state, the S_x state, between S_2 and S_1, resulting in the four-level scheme for the excited-state relaxation (Fig. 4B). The first experimental confirmation of an S_x state was provided by Koyama *et al.* (*14*, *15*). Using resonance Raman spectroscopy, this group located what they designated a $1^1B_u^-$ state between S_2 and S_1. This evidence was supported by time-resolved studies. Zhang *et al.* (*16*), studying excited-state dynamics of all-*trans*-neurosporene in the near infrared, needed to assume a four-level model to fit the experimental data by a singular-value decomposition algorithm. Yoshizawa *et al.* (*17*), studying the vibrational relaxation of S_1 of β-carotene by femtosecond time-resolved Raman spectroscopy, also required an additional state between S_2 and S_1 to fit their results. The time resolution used in these experiments (≈150 fs) did not allow this proposed intervening state to be directly observed.

With our enhanced temporal resolution, we have unequivocally resolved this intermediate state both in β-carotene and lycopene. We must now consider whether it is indeed a distinct electronic state or some relaxed form of S_2. For the following reasons, we favor the idea that this is a distinct electronic state. Our excitation pulse at 510-nm overlaps only the low-energy side of the carotenoids absorption band, thus enabling selective excitation of the zero-phonon line of the $S_0 \rightarrow S_2$ transition. Therefore, we expect only rather small vibrational relaxation to be possible. The large shift in the position of the transient differential transmission spectra of PA_2 and PA_x (Fig. 1) is incompatible with the expected small vibrational relaxation. In addition, vibrational relaxation would be expected to shift the PA_2 band to the blue, as observed for the PA_1 band (*17*, *18*), and not to the red (*24*). We note that the $S_2 \rightarrow S_x$ internal conversion process takes place on an extremely fast time scale, comparable to the periods of nuclear vibrations coupled to optical transitions, which are in the 20-fs range (*18*, *25*). Therefore the adiabatic approximation, commonly used to describe excited-state dynamics, fails and the reaction should be described as proceeding along a diabatic pathway linking the S_2 and S_x potential energy surfaces (*26*). A full molecular dynamics simulation rather than the simple rate equation model used in this work, would be required to satisfactorily describe this process.

Tavan and Schulten's calculations predicted that this intermediate state should be nonemissive. Our data, however, provide evidence that the S_x state in β-carotene is emissive (see trace at 560 nm in Fig. 2 and differential spectrum at 50-fs delay, showing stimulated emission). This reconciles our data with the previous fluorescence up-conversion experiments and explains why those experiments failed to identify the intermediate state, detecting an overlap of the fluorescence signals from S_2 and S_x. How can we explain the predictions of Tavan and Schulten that this new state should be nonemissive? Their calculations invoked strict selection rules based on perfect C_{2h} symmetry and noninteracting states. The S_x state could be activated by vibronic coupling with the S_2 state, due to their small energy difference. Another possibility, which we consider more likely, is that departure from the planar configuration, consequent to conformational rearrangement in the excited state after photoexcitation, may relax the spatial selection rules and thus activate emission from S_x.

The identification of an intermediate state in the energy relaxation of carotenoids has important implications for the understanding of the early events of photosynthesis. Until now, most of the extensive studies on the mechanism of light harvesting by carotenoids in photosynthesis have based their interpretations on the three-level model. These studies now need to be re-evaluated and repeated with sufficient time resolution to determine whether energy transfer from carotenoids to chlorophylls can take place from S_2 or S_x, or from a mixture of both. As an example, the carotenoid to bacteriochlorophyll transfer time in the LH2 antenna complex from the purple bacterium *Rhodopseudomonas aci-*

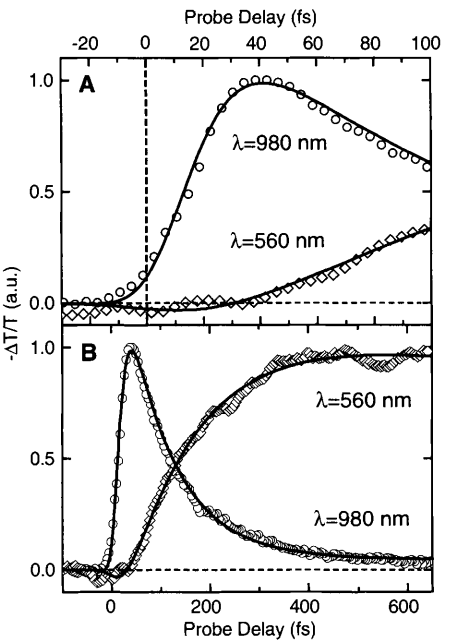

Fig. 3. (**A**) Circles show differential transmission dynamics in lycopene in cyclohexane solution at 980-nm probe wavelength (diamonds, at 560-nm) after photoexcitation by a 15-fs pulse resonant with the $S_0 \rightarrow S_2$ transition. Solid lines are fits using the four-state model described in the text. (**B**) Same data as (A) on a longer time scale.

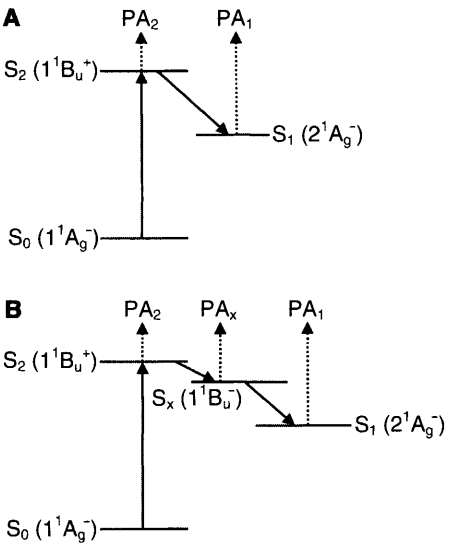

Fig. 4. Scheme of the three-state model (**A**) and the four-state model (**B**) used to describe excited-state dynamics of carotenoids.

dophila was determined to be 61 fs (*11*). The carotenoid in this complex, rhodopin glucoside, like lycopene has 11 conjugated double bonds. If we take the time scale for the S_2 to S_x transition from this report, then at least some of this energy transfer must involve S_x. Indeed, if S_2 was the only state from which energy transfer could occur, then the efficiency would be expected to be much lower than the measured value of this LH2 complex, which is 50%. This report illustrates again the remarkable subtlety of the photophysical behavior of carotenoids. The exact electronic designation of S_x and its involvement in the molecular mechanisms of carotenoid-to-chlorophyll singlet-singlet energy transfer remain to be determined.

References and Notes

1. O. Isler, *Carotenoids* (Birkhauser-Verlag, Basel, 1971).
2. H. A. Frank, R. J. Cogdell, *J. Photochem. Photobiol.* **63**, 257 (1996).
3. T. Ritz, A. Damjanovic, K. Schulten, J.-P. Zhang, Y. Koyama, *Photosynth. Res.* **66**, 125 (2000).
4. E. Hofmann *et al.*, *Science* **272**, 1788 (1996).
5. E. Pellegrin, J. Fink, S. L. Drechsler, *Phys. Rev. Lett.* **66**, 2022 (1991).
6. G. McDermott *et al.*, *Nature* **374**, 517 (1995).
7. A. Damjanovic, T. Ritz, K. Schulten, *Phys. Rev. E* **59**, 3293 (1999).
8. A. P. Shreve, J. K. Trautman, T. G. Owens, A. C. Albrecht, *Chem. Phys. Lett.* **178**, 89 (1991).
9. H. Kandori, H. Sasabe, M. J. Mimuro, *J. Am. Chem. Soc.* **116**, 2671 (1994).
10. A. N. Macpherson, T. Gillbro, *J. Phys. Chem. A* **102**, 5049 (1998).
11. A. N. Macpherson, J. B. Arellano, N. J. Fraser, R. J. Cogdell, T. Gillbro, *Biophys. J.* **80**, 923 (2001).
12. P. Tavan, K. Schulten, *J. Chem. Phys.* **85**, 6602 (1986).
13. ———, *Phys. Rev. B* **36**, 4337 (1987).
14. T. Sashima, H. Nagae, M. Kuki, Y. Koyama, *Chem. Phys. Lett.* **299**, 187 (1999).
15. T. Sashima, Y. Koyama, T. Yamada, H. Hashimoto, *J. Phys. Chem. B* **104**, 5011 (2000).
16. J.-P. Zhang, T. Inaba, Y. Watanabe, Y. Koyama, *Chem. Phys. Lett.* **332**, 351 (2000).
17. M. Yoshizawa, H. Aoki, H. Hashimoto, *Phys. Rev. B* **63**, R183301 (2001).
18. G. Cerullo, G. Lanzani, M. Zavelani-Rossi, S. De Silvestri, *Phys. Rev. B* **63**, R241104 (2001).
19. With respect to previously reported experiments (*18*), we have deliberately decreased the pump pulse bandwidth in order to reduce artefacts and avoid coherent oscillations, which are superimposed on the population dynamics.
20. G. Cerullo, M. Nisoli, S. Stagira, S. De Silvestri, *Opt. Lett.* **16**, 1283 (1998).
21. M. Zavelani-Rossi *et al.*, *Opt. Lett.* **26**, 1155 (2001).
22. Materials and methods are available as supporting material on *Science* Online.
23. J. P. Zhang, K. H. Skibsted, R. Fujii, Y. Koyama, *Photochem. Photobiol.* **73**, 219 (2001).
24. In order to explain the red shift of PA_x with respect to PA_2, a full spectroscopic characterization of the S_2 and S_x states, as well as the higher lying excited states, is required. A possible explanation could be that optical transitions starting from the two states reach different regions of the higher lying state potential energy surface. Due to strong energy dispersion of this surface, this would result in large difference of the vertical transition energy.
25. Y. Koyama, R. Fujii, in *The Photochemistry of Carotenoids*, H.A. Frank *et al.*, Eds. (Kluwer Academic Press, Netherlands, 1999), pp. 161–188.
26. Q. Wang, L. Peteanu, R. W. Schoenlein, C. V. Shank, R. Mathies, *Science* **266**, 422 (1994).

27. We are indebted to C. Manzoni for help in developing the experimental setup. R.J.C. thanks the UK Biotechnology and Biological Sciences Research Council (BBSRC) for support. R.J.C. acknowledges support from the European Community – Access to Research Infrastructure action of the improving Human Potential Programme, contract N. HPRI-CT-2001-00148 (Center For Ultrafast Science and Biomedical Optics, CUSBO). H.H. thanks the Japanese Ministry of Education, Culture, Sports, Science and Technology for financial support.

Supporting Online Material
www.sciencemag.org/cgi/content/full/298/5602/2395/DC1
Materials and Methods
Fig. S1
References and Notes

4 June 2002; accepted 7 November 2002

Rates of Behavior and Aging Specified by Mitochondrial Function During Development

Andrew Dillin,[1]* Ao-Lin Hsu,[1] Nuno Arantes-Oliveira,[1]† Joshua Lehrer-Graiwer,[1] Honor Hsin,[1]‡ Andrew G. Fraser,[2] Ravi S. Kamath,[2] Julie Ahringer,[2] Cynthia Kenyon[1]§

To explore the role of mitochondrial activity in the aging process, we have lowered the activity of the electron transport chain and adenosine 5′-triphosphate (ATP) synthase with RNA interference (RNAi) in *Caenorhabditis elegans*. These perturbations reduced body size and behavioral rates and extended adult life-span. Restoring messenger RNA to near-normal levels during adulthood did not elevate ATP levels and did not correct any of these phenotypes. Conversely, inhibiting respiratory-chain components during adulthood only did not reset behavioral rates and did not affect life-span. Thus, the developing animal appears to contain a regulatory system that monitors mitochondrial activity early in life and, in response, establishes rates of respiration, behavior, and aging that persist during adulthood.

During a systematic screen of a *C. elegans* chromosome I RNAi library (*1*, *2*), we found that animals grown on bacteria expressing double-stranded RNA (dsRNA) encoding a component of the mitochondrial ATP synthase (*atp-3*) lived much longer than normal (*3*) (Fig. 1A, table S1). RNAi of three genes encoding respiratory-chain components also extended life-span: *nuo-2*, which encodes a component of complex I (NADH/ubiquinone oxidoreductase); *cyc-1*, which encodes a component of complex III (cytochrome c reductase); and *cco-1*, which encodes a component of complex IV (cytochrome c oxidase) (Fig. 1A, table S1) (*3*). Treatment of wild-type animals with antimycin A, which inhibits complex III (*4*), increased life-span as well (*3*) (Fig. 1D, table S1).

RNAi of respiratory-chain components also affected growth and behavior. The animals were smaller than normal. They were well proportioned (fig. S1, table S2) and did not have an obvious decrease in cell number. We counted cells in two postembryonic lineages, the vulval and epidermal seam cell lineages (*5*), and found that cell number was normal (*3*). Thus, in these tissues (and likely in others as well), a metabolite whose level is regulated by mitochondrial respiration acts as a signal to control cell size. Small body size itself is unlikely to extend life-span, because mutants defective in *daf-4*, which encodes a transforming growth factor–β type II receptor (*6*), are small but not long-lived (*7*). Respiratory-chain RNAi also decreased the rate of growth to adulthood, as well as the rates of pharyngeal pumping (eating) and defecation (table S2). In addition, the animals moved more slowly than normal (table S2).

Inhibition of a component of respiratory chain complex III, *isp-1*, in *C. elegans* has been shown to reduce oxygen consumption (*8*). Inhibiting respiratory-chain components and ATP synthase would also be predicted to reduce ATP levels. We found that ATP levels were reduced 60 to 80% in animals subjected to *cyc-1* (complex III) or *atp-3* (ATP synthase) RNAi and 40 to 60% in animals treated with *nuo-2* (complex I) or *cco-1* (complex IV) RNAi (*3*) (Fig. 2).[6] These findings, and the fact that all these proteins are known to function together in the processes of respiration and ATP production, suggest that reducing the rates of respira-

[1]Department of Biochemistry and Biophysics, University of California, San Francisco, CA 94143–0448, USA. [2]Wellcome/CRC Institute, University of Cambridge, Tennis Court Road, Cambridge CB21QR, UK.

*Present address: The Salk Institute for Biological Studies, Molecular and Cell Biology Laboratory, La Jolla, CA 92037, USA.

†Present address: IN+ Center for Innovation, Technology and Policy Research Instituto Superior Técnico, Technical University of Lisbon 1049-001, Lisbon, Portugal.

‡Present address: Harvard University, Cambridge, MA 02115, USA.

§To whom correspondence should be addressed. E-mail: ckenyon@biochem.ucsf.edu